

Equilibrium and non-equilibrium dynamics of the sub-ohmic spin-boson model

Frithjof B. Anders,¹ Ralf Bulla,² and Matthias Vojta³

¹*Fachbereich Physik, Universität Bremen, 28334 Bremen, Germany*

²*Theoretische Physik III, Elektronische Korrelationen und Magnetismus, Universität Augsburg, 86135 Augsburg, Germany*

³*Institut für Theoretische Physik, Universität zu Köln, Zùlpicher Str. 77, 50937 Köln, Germany*

(Dated: April 2, 2007)

Employing the non-perturbative numerical renormalization group method, we study the dynamics of the spin-boson model, which describes a two-level system coupled to a bosonic bath with spectral density $J(\omega) \propto \omega^s$. We show that, in contrast to the case of ohmic damping, the delocalized phase of the sub-ohmic model cannot be characterized by a single energy scale only, due to the presence of a non-trivial quantum phase transition. In the strongly sub-ohmic regime, $s \ll 1$, weakly damped coherent oscillations on short time scales are possible even in the *localized* phase – this is of crucial relevance, e.g., for qubits subject to electromagnetic noise.

Models of quantum dissipation [1, 2] have gained significant attention over the last years, due to their wide range of applications from the effect of friction on the electron transfer in biomolecules [3] to the description of the quantum entanglement between a qubit and its environment [4, 5] (for further applications see Refs. 1, 2).

The simplest quantum-dissipative models belong to the class of impurity models and consist of a small quantum system coupled to a bath of harmonic oscillators. One familiar bosonic impurity model is the spin-boson model,

$$H = -\frac{\Delta}{2}\sigma_x + \frac{\epsilon}{2}\sigma_z + \sum_i \omega_i a_i^\dagger a_i + \frac{\sigma_z}{2} \sum_i \lambda_i (a_i + a_i^\dagger). \quad (1)$$

It describes a generic two-level system, represented by the Pauli matrices σ_j , which is linearly coupled to a bath of harmonic oscillators, with creation operators a_i^\dagger and frequencies ω_i . The bare tunneling amplitude between the two spin states $|\uparrow\rangle, |\downarrow\rangle$ is given by Δ , and ϵ is an additional bias (which is zero in the following, except for the preparation of the initial state as discussed below). The coupling between spin and bosonic bath is specified by the bath spectral function $J(\omega) = \pi \sum_i \lambda_i^2 \delta(\omega - \omega_i)$. The asymptotic low-temperature behavior is determined by the low-energy part of the spectrum. Discarding high-energy details, the standard parametrization is

$$J(\omega) = 2\pi \alpha \omega_c^{1-s} \omega^s, \quad 0 < \omega < \omega_c, \quad s > -1 \quad (2)$$

where the dimensionless parameter α characterizes the dissipation strength, and ω_c is a cutoff energy.

In case of ohmic dissipation, $s = 1$, a quantum transition of Kosterlitz-Thouless type separates a localized phase at $\alpha \geq \alpha_c$, displaying a doubly degenerate ground state, from a delocalized phase at $\alpha < \alpha_c$ with a unique ground state [1, 2]. The delocalized regime is characterized by a finite effective tunnel splitting, Δ_r , between the two levels, whereas the tunnel splitting renormalizes to zero in the localized phase. For $\Delta \ll \omega_c$ the transition occurs at $\alpha_c = 1$.

The sub-ohmic case, $s < 1$, [5, 6, 7, 8, 9] turns out to be different. For $\Delta/\omega_c \rightarrow 0$ the system is localized for

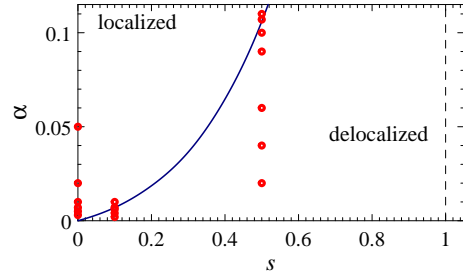


FIG. 1: Zero-temperature phase diagram of the spin-boson model from NRG [23], for fixed $\Delta = 0.1$ and $\omega_c = 1$. The axes denote the bath exponent s and the dissipation strength α . The circles indicate the parameter values for which results will be presented in this paper.

any non-zero coupling [1, 2], but for large Δ a delocalized phase was argued to exist [6, 7]. We have recently [8] shown, using an extension of the non-perturbative Numerical Renormalization Group (NRG), that a *continuous* quantum phase transition (QPT) occurs for *all* $0 < s < 1$, in contrast to earlier proposals [6]. The numerically determined equilibrium phase diagram is shown in Fig. 1.

Detailed studies of non-equilibrium properties, like the quantity $P(t) = \langle \sigma_z(t) \rangle$ for a spin initially prepared in the $|\uparrow\rangle$ state, have mainly covered the ohmic damping case for small Δ [1, 10, 11]. Here, weakly damped oscillations can only be observed for $\alpha < 1/2$, whereas $1/2 < \alpha < 1$ leads to overdamped behavior, i.e., exponential decay of $P(t)$ to zero. Finally, in the localized phase, $\alpha > 1$, $P(t)$ decays to a finite value. Studies of the dynamics in the sub-ohmic case have so far been restricted to the use of perturbative methods [12]. Considering that these miss the QPT and the localized phase present for $s < 1$, the validity of the corresponding results is questionable.

The purpose of this paper is to provide non-perturbative results for the dynamics of the sub-ohmic spin-boson model, for the whole range of model parameters. Our main results can be summarized as follows: Whereas the delocalized phase of the ohmic model is

dominated by a single energy scale, Δ_r , only, the sub-ohmic model is more complicated due to the presence of a second-order QPT. Near the transition a quantum critical (QC) crossover scale T^* appears [8], which – in the strongly sub-ohmic regime – co-exists with a larger scale Δ_r that can still be identified with the renormalized tunnel splitting. As we demonstrate below, T^* vanishes at the transition to the localized phase, whereas Δ_r stays finite. The latter fact is crucial for the non-equilibrium dynamics: we find the presence of coherent weakly damped oscillations, with frequency Δ_r , even in the localized phase, $\alpha > \alpha_c$, for $s \ll 1$. This is particularly relevant for the case $s = 0$, related to so-called $1/f$ noise in an electromagnetic environment. Here, the equilibrium spin-boson model is always in the localized phase, however, coherent oscillations are still possible for small α and short times.

NRG. We employ Wilson’s NRG method [13] to study the sub-ohmic spin-boson model, utilizing two recently developed extensions: (i) Refs. 8, 14 generalized the NRG at thermodynamic equilibrium to impurity models with a *bosonic* bath. (ii) Ref. 15 proposed an algorithm to study non-equilibrium dynamics in real time and applied it to the Anderson and Kondo models. (For an earlier non-equilibrium NRG approach see Ref. 16.) The time-dependent NRG provides a spectral representation of the time-independent Hamiltonian H^f , governing the time evolution for $t > 0$, at all energy scales using a complete basis set, and expresses the real-time dynamics of observables in terms of a summation over reduced density matrices [15]. The latter contain all information on decoherence and dissipation. Two independent bosonic NRG runs [14] are required, one for the initial density matrix and the other for the approximate eigenbasis of H^f . In order to accurately simulate the continuum limit with a NRG chain of finite length, we average over N_Z different bath discretizations for a fixed discretization parameter Λ . All numerical results below are for temperature $T = 0$, unless otherwise noted.

Renormalization group flow and crossovers. To set the stage, we summarize the renormalization group flow of the spin-boson model [8, 14, 17]. In the following, the terms localized (delocalized) are defined through the impurity entropy [14, 18] being $\ln 2$ (zero). Note that this has to be contrasted with localization in the sense that a system initially prepared with the impurity spin in one specified direction remains in this spin state under time evolution. For any finite temperature, thermal excitations destroy localization in this sense (see Ref. 1). For a discussion of this point, in particular the connection between NRG flow and thermodynamic properties, see Secs. III and IV in Ref. 14.

In the ohmic case, the flow for $\alpha < \alpha_c$ is from the localized towards the delocalized phase (upon lowering the energy), with Δ_r being the crossover energy scale. Thus the behavior for energies or temperatures below

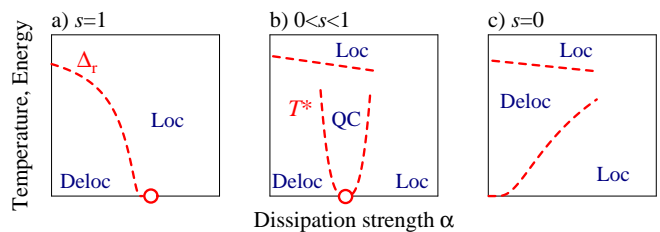


FIG. 2: Schematic crossover diagrams for the spin-boson model for different bath exponents s , deduced from NRG, with regimes of localized, delocalized, and quantum critical (QC) behavior. The open dots denote QPTs, for details see text. (Note that the α scale is different for the three panels.)

Δ_r is delocalized, Fig. 2a.

For $0 < s < 1$ the critical fixed point controls the physics of the QC region. It is bounded by crossover lines $T^* \propto |\alpha - \alpha_c|^\nu$ and covers a large portion of the phase diagram due to the large value of the correlation length exponent ν , Fig. 2b. (In fact, ν diverges both as $s \rightarrow 1^-$ and $s \rightarrow 0^+$ [17].) The critical fixed point merges with the localized (delocalized) one as $s \rightarrow 1^-$ ($s \rightarrow 0^+$), implying that the characteristics of the QC regime becomes more “delocalized” as s is decreased towards zero. For s not too close to 1 there also is a distinct crossover from the high-temperature localized regime ($T \gg \Delta$) to the delocalized or critical regimes.

Consequently, for $s = 0$ and small α the flow is first from localized to delocalized, with a crossover scale Δ_r , finally to the localized fixed point (which controls the ground state for any α) – the latter crossover is characterized by the scale T^* , with $T^* \sim \omega_c \exp(-\Delta/\alpha\omega_c)$. As shown in Fig. 2c, the low-energy crossover at $s = 0$ is thus opposite to the one at $s = 1$!

In general, we may expect coherent, weakly damped dynamics, with a rate Δ_r , in the delocalized regime (and in the QC one for small s as well).

Equilibrium dynamics. Let us focus on the Fourier transform $C(\omega)$ of the symmetrized equilibrium correlation function $C(t) = \frac{1}{2} \langle [\sigma_z(t), \sigma_z]_+ \rangle$. We start by noting the low-frequency asymptotics: In the delocalized phase $C(\omega) \propto \omega^s$ [6, 19], whereas in the localized phase $C(\omega)$ displays a $A\delta(\omega)$ contribution, which reflects the doubly degenerate ground state, and A plays the role of an order parameter (equivalent to the thermodynamic expectation value $\langle \sigma_z \rangle$). Turning to the finite-frequency behavior, our numerics for $s = 1$ reproduces the well-known results (see Sec. V in Ref. 14), i.e., $C(\omega)$ is dominated by a single peak at Δ_r which shifts to lower frequencies with increasing α and disappears at the transition, $\alpha = \alpha_c$. (Results for s down to 0.8 are qualitatively similar.)

For smaller s the influence of the critical fixed point becomes increasingly visible, see Fig. 3a for $s = 0.5$. For small α we observe that $C(\omega)$ is dominated by a peak close to Δ , as expected. However, with increasing

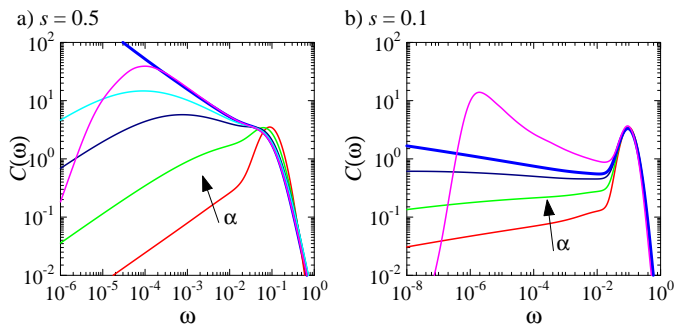


FIG. 3: Equilibrium spin correlation function $C(\omega)$ for a) $s = 0.5$ and $\alpha = 0.02, 0.06, 0.09, 0.10, 0.107, 0.11$; b) $s = 0.1$ and $\alpha = 0.002, 0.004, 0.006, 0.007, 0.01$; the thick curves are very close to the critical point (for $s = 0.5$ we find $\alpha_c = 0.1065$ and $s = 0.1$, $\alpha_c = 0.0071$). The curves correspond to the parameter values shown as circles in Fig. 1. (The peak width at small α is an artifact of the NRG broadening.)

α weight is transferred to smaller frequencies, leaving a shoulder feature close to Δ intact. For $\alpha \lesssim \alpha_c$, $C(\omega)$ has a pronounced peak at $\omega \sim T^*$ – this peak separates the QC divergence $C(\omega) \propto \omega^{-s}$ at intermediate energies from the low-energy ω^s behavior. At criticality, $T^* \rightarrow 0$, and $C(\omega) \propto \omega^{-s}$ down to lowest energies.

A further decrease of the bath exponent s – see Fig. 3b for $s = 0.1$ – shows that the high-frequency peak in the vicinity of Δ is suppressed more slowly upon increasing α , reflecting the fact that the QC behavior is more “de-localized” for small s . In particular, this peak, which is usually taken as indication for the presence of coherent weakly damped dynamics, survives even for $\alpha > \alpha_c$ (!).

Fig. 4 for $s = 0$ illustrates this fact: here the ground state is localized for any s , but a well-defined peak at Δ_r is visible for all $\alpha < 0.05$ (for $\Delta/\omega_c = 0.1$). Further, there is a low-energy peak at T^* for small α , in addition to the $A\delta(\omega)$ contribution (not plotted) characteristic of the localized phase.

Parenthetically, we note that the low-energy part of $C(\omega, T)$ near $\alpha = \alpha_c$ is expected to show universal scal-

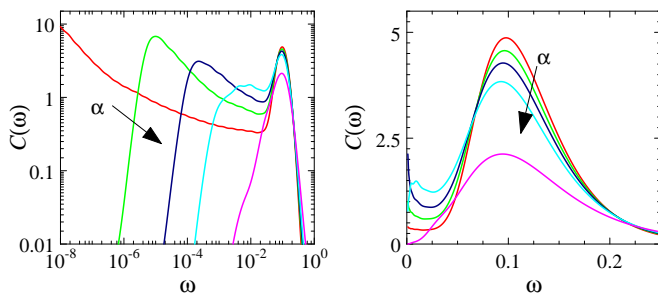


FIG. 4: Equilibrium spin correlation function $C(\omega)$ for $s = 0$ and $\alpha = 0.003, 0.005, 0.007, 0.01, 0.02$. Both panels show the same data, but the right one has a linear ω scale. The $A\delta(\omega)$ contribution is not shown.

ing behavior, including ω/T scaling, as the critical fixed point obeys hyperscaling properties for all $0 < s < 1$ [17].

Non-equilibrium dynamics. We now present results for $P(t)$, obtained with the non-equilibrium generalization of the NRG [15]. The spin is prepared in the $|\uparrow\rangle$ state, by calculating the equilibrium density matrix of the initial Hamiltonian H^i with a large spin polarization energy $\epsilon/\omega_c = 100$ and $\Delta = 0$. At $t = 0$, ϵ is switched off, and Δ is set to $\Delta/\omega_c = 0.1$. This defines H^f , governing the time evolution of the initial density operator.

Fig. 5 shows $P(t)$ for $s = 0.5$, $\Delta/\omega_c = 0.1$, and various values of α . For weak coupling, i.e. $\alpha \ll \alpha_c$, a damped oscillatory behavior is found. Increasing α suppresses the oscillations at longer time scales but maintains the initial ones. A very shallow oscillation at short times can be seen even for $\alpha > \alpha_c$ which is consistent with the $C(\omega)$ data presented in Fig. 3. For $\alpha > \alpha_c$ $P(t)$ shows only a very weak time dependence for intermediate times and is expected to approach a finite value $P(\infty)$ for $t \rightarrow \infty$, an indication of localization (see below).

Let us now turn to $s = 0$, Fig. 6. Even though any finite value of α places the model in the localized phase in equilibrium, the non-equilibrium dynamics of $P(t)$ clearly exhibits oscillatory behavior for small α . Roughly speaking, the time evolution mimics the RG flow and thus corresponds to a reduction of temperature in the phase diagram Fig. 2c: At short times the physics is governed by the delocalized fixed point; it crosses over to the localized fixed point at long time scales. Upon increasing α the time scale of the crossover from oscillatory to damped behavior in $P(t)$ is reduced, consistent with the low-temperature crossover line in Fig. 2c.

For small damping, the decay of the $P(t)$ oscillations is exponential. Comparing the decay rate with the popular Bloch-Redfield approach [20] gives deviations of less than 10% for $s = 0.1$, $\alpha = 0.002$, but the agreement becomes worse for larger α or smaller s . For all $s < 1$ we observe that with increasing α the frequency of the initial oscillations in $P(t)$ first decreases (consistent with the result of straightforward perturbation theory), but for larger α and small s then slightly increases with α , indicating that one leaves the perturbatively accessible regime. [$C(\omega)$ in Figs. 3, 4 is inconclusive w.r.t. the peak position due to the logarithmic broadening with the NRG.]

The long-time limit $P(\infty)$ measures the “degree of localization”, equivalent to the order parameter $\langle \sigma_z \rangle$ in equilibrium [and proportional to the A -coefficient of the $\delta(\omega)$ contribution to $C(\omega)$]. $P(\infty)$ vanishes continuously at the transition for any $0 \leq s < 1$. [For the smallest value of α shown in Fig. 6 for $s = 0$ ($\alpha = 0.003$), the $P(t)$ oscillates around $P(\infty) \approx 0.1$.] Note the difference to the ohmic case, $s = 1$, where $P(\infty)$ jumps from a finite value for $\alpha > \alpha_c$ to zero $\alpha < \alpha_c$.

A few remarks are in order. On general grounds, one may expect a power-law decay in the long-time limit of $P(t)$ at the critical point, $\alpha = \alpha_c$, for all $0 < s < 1$. This

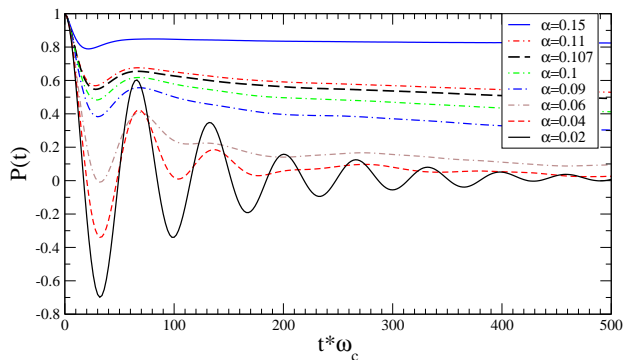


FIG. 5: Time evolution of $P(t)$ for $s = 0.5$, $\Delta/\omega_c = 0.1$, and various values of α ($\alpha_c = 0.1065$).

power law will be cutoff away from criticality, on a time scale $\propto 1/T^*$. At present, the accuracy of the numerical data in non-equilibrium is not sufficient to verify this. Since the short-time behavior of $P(t)$ is dominated by the high-energy properties, i.e., by Δ_r , small but finite temperatures do not alter the response on time scales shown in Figs. 5 and 6. At finite T we only observe a decay of $P(t)$ to zero for long times and parameters corresponding to the localized phase (not shown).

Summary. We have studied the dynamics of the sub-ohmic spin-boson model, both in equilibrium and non-equilibrium, using non-perturbative numerical renormalization group techniques. The model displays a continuous QPT for all bath exponents $0 < s < 1$, and this leads to highly non-trivial dynamical properties. In contrast to the ohmic situation, the sub-ohmic case cannot be characterized by a single energy scale only. This is particularly striking for $s \ll 1$: while the low-energy, long-time behavior is dominated by the presence of nearly critical fluctuations over a large regime of parameters, the behavior at short times or elevated energies derives from weakly renormalized tunneling, which can be coherent even in situations with a localized thermodynamic ground state.

Our results imply that perturbative methods, only cap-

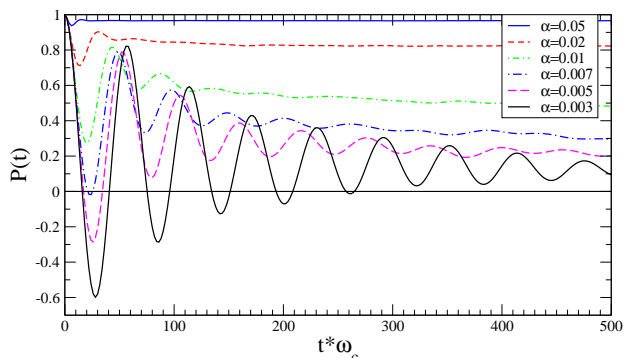


FIG. 6: Time evolution of $P(t)$ for $s = 0$, $\Delta/\omega_c = 0.1$, and various values of α ($\alpha_c = 0$ here).

turing the renormalized coherent tunneling, may be applied to the sub-ohmic model at short times, but clearly fail in the long-time limit. Furthermore, approximations aiming on a description of the spin-boson physics in terms of a single energy scale Δ_r only, as done in Refs. 6, 9, are not applicable in the strongly sub-ohmic regime. Last not least, let us emphasize that the sub-ohmic situations of $s = 1/2$ and $s = 0$ are of immediate experimental relevance, e.g. for the description of electromagnetic transmission lines [21] and general $1/f$ noise, respectively. Furthermore, $s = 1/2$ baths may be realized in the context of effective impurities in ultracold gases [22].

We thank S. Kehrein, S. Kohler, A. Rosch, S. Tornow, and W. Zwerger for discussions, and A. Schiller and N.-H. Tong for collaborations on related work. This research was supported by the DFG through AN 275/5-1 (FBA), SFB 484 (RB), SFB 608 (MV), as well as the NIC, FZ Jülich under project no. HHH000 (FBA).

-
- [1] A. J. Leggett *et al.*, Rev. Mod. Phys. **59**, 1 (1987).
 - [2] U. Weiss, *Quantum dissipative systems*, World Scientific, Singapore (1999).
 - [3] A. Garg *et al.*, J. Chem. Phys. **83**, 4491 (1985).
 - [4] M. Thorwart and P. Hänggi, Phys. Rev. A **65**, 012309 (2001); M. J. Storcz and F. K. Wilhelm, *ibid.* **67**, 042319 (2003).
 - [5] D. V. Khveshchenko, Phys. Rev. B **69**, 153311 (2004).
 - [6] S. Kehrein and A. Mielke, Phys. Lett. A **219**, 313 (1996).
 - [7] H. Spohn and R. Dümcke, J. Stat. Phys. **41**, 389 (1985).
 - [8] R. Bulla *et al.*, Phys. Rev. Lett. **91**, 170601 (2003).
 - [9] A. Chin and M. Turlakov, Phys. Rev. B **73**, 075311 (2006).
 - [10] T. A. Costi and C. Kieffer, Phys. Rev. Lett. **76**, 1683 (1996).
 - [11] M. Keil and H. Schoeller, Phys. Rev. B **63**, 180302(R) (2001).
 - [12] A. Shnirman and G. Schön, in: *Quantum Noise in Mesoscopic Physics*, ed. Yu. Nazarov, Kluwer, Dordrecht (2003).
 - [13] K. G. Wilson, Rev. Mod. Phys. **47**, 773 (1975); R. Bulla, T. Costi, and Th. Pruschke, cond-mat/0701105.
 - [14] R. Bulla *et al.*, Phys. Rev. B **71**, 045122 (2005).
 - [15] F. B. Anders and A. Schiller, Phys. Rev. Lett. **95**, 196801 (2005) and Phys. Rev. B **74**, 245113 (2006).
 - [16] T. A. Costi, Phys. Rev. B **55**, 3003 (1997).
 - [17] M. Vojta *et al.*, Phys. Rev. Lett. **94**, 070604 (2005).
 - [18] Impurity entropy is defined as the impurity contribution to the thermodynamic entropy of the model (1).
 - [19] H. Spohn and W. Zwerger, J. Stat. Phys. **94**, 1037 (1999).
 - [20] V. May and O. Kühn, *Charge and Energy Transfer Dynamics in Molecular Systems*, Wiley-VCH, Berlin (2000).
 - [21] G. L. Ingold and Yu. V. Nazarov, in: *Single Charge Tunneling*, eds. H. Grabert and M. H. Devoret, Plenum Press, New York (1992).
 - [22] W. Zwerger, private communication, see also: A. Recati *et al.*, cond-mat/0212413 and Phys. Rev. Lett. **94**, 040404 (2005).
 - [23] The NRG parameters are: $\Lambda = 2$, $N_s = 100$, $N_b = 8$, $N_{b0} =$

100. The non-equilibrium calculations employ $N_Z = 32$ and no additional damping, see Ref. 15 for details.